Cerebral Cortex, May 2016;26: 1965–1974

doi: 10.1093/cercor/bhv013
Advance Access Publication Date: 6 February 2015
Original Article

ORIGINAL ARTICLE

A Working Memory Buffer in Parahippocampal Regions: Evidence from a Load Effect during the Delay Period

Karin Schon[1,2,3,4,5,†], Randall E. Newmark[1,2,3,5,†], Robert S. Ross[1,3,5], and Chantal E. Stern[1,2,3,5]

[1]Department of Psychological and Brain Sciences, Center for Memory and Brain, [2]Graduate Program for Neuroscience, [3]CELEST, Center of Excellence for Learning in Education, Science, and Technology, Boston University, Boston, MA 02215, USA, [4]Department of Anatomy and Neurobiology, Boston University School of Medicine, Boston, MA 02118, USA, and [5]Athinoula A. Martinos Center for Biomedical Imaging, Massachusetts General Hospital, Charlestown, MA 02129, USA

Address correspondence to Karin Schon, Center for Memory and Brain, Boston University, 2 Cummington Mall, Boston, MA 02215, USA.
Email: kschon@bu.edu

[†]Drs. Schon and Newmark contributed equally to this article and share joint first authorship.

Abstract

Computational models have proposed that the entorhinal cortex (EC) is well suited for maintaining multiple items in working memory (WM). Evidence from animal recording and human neuroimaging studies show that medial temporal lobe areas including the perirhinal (PrC), EC, and CA1 hippocampal subfield may contribute to active maintenance during WM. Previous neuroimaging work also suggests CA1 may be recruited transiently when encoding novel information, and EC and CA1 may be involved in maintaining multiple items in WM. In this study, we tested the prediction that a putative WM buffer would demonstrate a load-dependent effect during a WM delay. Using high-resolution fMRI, we examined whether activity within the hippocampus (CA3/DG, CA1, and subiculum) and surrounding medial temporal cortices (PrC, EC, and parahippocampal cortex—PHC) is modulated in a load-dependent manner. We employed a delayed matching-to-sample task with novel scenes at 2 different WM loads. A contrast between high- and low-WM load showed greater activity within CA1 and subiculum during the encoding phase, and greater EC, PrC, and PHC activity during WM maintenance. These results are consistent with computational models and suggest that EC/PrC and PHC act as a WM buffer by actively maintaining novel information in a capacity-dependent manner.

Key words: encoding, high-resolution fMRI, hippocampus, maintenance, matching-to-sample

Introduction

Theoretical models have proposed that the entorhinal cortex (EC) supports the active maintenance of multiple items during working memory (WM) (Jensen and Lisman 2005; Koene and Hasselmo 2007). These entorhinal buffer models have proposed that sustained activity in the EC during active maintenance (persistent spiking in single-unit recordings in rodents) could provide a buffer for WM that can facilitate hippocampus-dependent encoding into long-term memory (Lisman and Idiart 1995; Jensen and Lisman 1996; Koene et al. 2003; McGaughy et al. 2005). These models state that intrinsic calcium-dependent afterdepolarization currents are activated by cholinergic innervation of EC neurons. The intrinsic currents support persistent spiking when synaptic representations outside the medial temporal lobes (MTLs) do not exist, as is the case for novel stimuli. Support for

this entorhinal buffer model comes from McGaughy et al. (2005), who have shown that cholinergic deafferentation of entorhinal neurons in the rat impairs delayed nonmatching to sample for novel odors, but not for familiar odors after a 15-min delay. Evidence from unit recordings in monkeys and rats has shown stimulus-selective and nonselective sustained neuronal firing in EC neurons during the delay period of delayed-match-to-sample and delayed nonmatch-to-sample tasks (Suzuki et al. 1997; Young et al. 1997) that is distractor resistant (Suzuki et al. 1997). Following depolarization, persistent firing in the absence of stimulus input has been observed not only within the EC (Klink and Alonso 1997; Fransén et al. 2004; Tahvildari et al. 2007; Yoshida et al. 2008), but also in the perirhinal cortex (PrC) (Navaroli et al. 2012), the CA3 subfield (Jochems and Yoshida 2013), and CA1 subfield (Knauer et al. 2013). Functional neuroimaging studies have reported delay-period activity in EC, PrC, parahippocampal cortex (PHC), and hippocampus during WM tasks (Pessoa et al. 2002; Schon et al. 2004, 2013; Nichols et al. 2006; Olsen et al. 2009; Newmark et al. 2013), and it has been shown that this delay-period activity can support long-term encoding (Schon et al. 2004; Ranganath et al. 2005; Nichols et al. 2006), short-term encoding during WM (Pessoa et al. 2002; Olsen et al. 2009), novelty detection (Ranganath and Esposito 2001; Schon et al. 2013), and encoding/processing of item similarity, consistent with a proposed pattern separation or disambiguation process (Newmark et al. 2013). In particular, Olsen et al. (2009) demonstrated sustained delay-period activity in EC, PrC, and anterior hippocampus suggestive of short-term stimulus maintenance that is independent from novelty encoding, whereas delay-period activity in the PHC showed a linear increase suggestive of an anticipatory process. Similarly, while not directly examining delay-period activity, Fernández et al. (1999) have shown that sustained EC activity is correlated with subsequent cued recall. Recently, we have shown delay-period activity in CA1 and EC when multiple stimuli with overlapping features are maintained (Newmark et al. 2013).

Anatomically, the EC is ideally suited as a buffer for WM, because of its well-established role as a major interface between the hippocampus and cortical areas. It receives projections from unimodal and polysensory cortical areas via the perirhinal and parahippocampal cortices and from orbitofrontal and dorsolateral prefrontal cortex among other regions (Van Hoesen and Pandya 1975a; Insausti et al. 1987; Suzuki and Amaral 1994). In a prominent hierarchical model of the organization of the cerebral cortex based on anatomical studies, the EC, together with the hippocampus, sit on top of the visual information flow hierarchy (Felleman and Van Essen 1991). The EC relays incoming information to the hippocampus and has direct projections to the DG, CA1, and CA3 subfields of the hippocampus (Van Hoesen and Pandya 1975b; Witter et al. 1989).

Together, this work suggests that CA1 along with EC and PrC may act as a WM buffer. Critical features of a WM buffer are the co-existence of LTM processes, observed, for example, using a subsequent memory paradigm (Fernández et al. 1999; Schon et al. 2004), and WM processes during the delay period, such as active maintenance that is distractor resistant (Suzuki et al. 1997) or that is modulated by WM load. In this study, we test the prediction that the WM buffer should show a load-dependent effect during a WM task delay, that is, delay-period activity should be modulated by the number of new items held in WM.

WM load-modulated delay-period activity in the MTL, specifically in the hippocampus, has not consistently been observed in whole-brain fMRI studies (Zarahn et al. 2005; Axmacher et al. 2007; Schon et al. 2009; Kochan et al. 2011). This may be because whole-brain studies rely on standard normalization techniques that are often unable to show activity differences in small regions, such as CA1, or in regions with highly variable anatomical boundaries, such as those between EC and PrC. Recent investigations in patients with MTL damage have suggested that the hippocampus in particular should only be recruited when WM capacity is exceeded (Shrager et al. 2008; Jeneson et al. 2010) or when active maintenance is impaired through distraction (Shrager et al. 2008). These results remain inconclusive, however, because patient studies cannot distinguish between transient contributions to encoding and sustained contributions during the WM delay.

Another potential candidate for the WM buffer may be a region of the PHC given the PHC's well-established role in scene processing (Epstein et al. 2007) and mnemonic encoding of novel visuospatial scenes (Epstein et al. 1999; Schon et al. 2004; Awipi and Davachi 2008; Preston et al. 2010) and of contextual information (Diana et al. 2007; Staresina et al. 2011). Critical for a WM buffer role, in addition to a role in mnemonic encoding during the WM delay, is that this region should also show sustained activity during brief WM delays that is greater with greater mnemonic load. Using a delayed matching-to-sample task with unfamiliar scenes, we have shown that delay-period activity in the PHC is associated with subsequent scene memory, suggesting that this region supports encoding of novel scenes during the WM task delay (Schon et al. 2004). However, while previous fMRI studies with two-back task designs have shown greater PHC activity with greater WM load of spatially complex stimuli (2-back > 1-back; Lee and Rudebeck 2010), so far there is limited evidence that the PHC region is modulated by stimulus load during the WM task delay (Ranganath et al. 2004; Axmacher et al. 2009). Ranganath et al. (2004) showed that a load effect in this region during the WM task delay was absent. In contrast, Axmacher and colleagues observed greater activity in the PHC with "lower" load. Together, these studies suggest the PHC may not be the locus of the WM buffer. Given this region's role in scene processing and mnemonic encoding, we also examined whether activity in the PHC was modulated by WM load. However, based on the existing literature, we did not have a specific hypothesis regarding this region's role as a WM buffer.

Here, we have extended our previous work (Schon et al. 2009; Newmark et al. 2013) by using high-resolution fMRI and cross-participant alignment methods optimized for small ROIs (Stark and Okado 2003; Miller et al. 2005; Yassa and Stark 2009) to differentiate the functional contributions of hippocampal subfields and parahippocampal regions to WM maintenance at high and low loads. We predicted that EC and PrC would show increased activity with higher WM loads during task delay. We also investigated CA1 and PHC activity during the encoding phase and delay period. We hypothesized that if CA1 and PHC activity was modulated by WM load during the delay, this would suggest a role for CA1 and PHC as a buffer during WM maintenance. Alternatively, if CA1 showed increased transient activity during the encoding phase only, this, together with findings from our previous work (Schon et al. 2004), may suggest long-term encoding or visual information processing during WM.

Materials and Methods

Participants

We recruited 18 participants (mean age: 20.0 ± 2.0 years, 10 female) from the Boston University community and surrounding area. Participants gave informed written consent, and the study

was approved by both the Partners Human Research Committee and the Boston University Charles River Campus Institutional Review Board. All subjects had normal or corrected vision, and all reported no history of neurologic or psychiatric disorders and had no counter indicators for MR imaging. Three participants were excluded from analyses due to excessive motion and technical difficulties during scanning.

Task Procedure

Stimuli consisted of 360 color photographs of unfamiliar trial-unique visual outdoor scenes. Stimuli, task design, and procedures were identical to those used previously in our whole-brain fMRI study (Schon et al. 2009). During fMRI scanning, subjects performed a Sternberg task (Sternberg 1966) in which 2 or 4 scenes (Load 2 and Load 4) were sequentially shown (sample; average duration per scene: 1600 ms followed by a blank screen, average duration: 400 ms, see Schon et al. 2009; followed by a variable-length delay period, maintenance: 4, 6, or 8 s; followed by a probe scene, test: 2 s, and a variable intertrial interval: 8, 10, or 12 s; Fig. 1). As in our previous study, sample scene presentations were variable in duration (mean, 1600 ms; range, 1400–1800 ms) and were followed by a temporal jitter (mean, 400 ms; range, 200–600 ms, uniform distribution in steps of 100 ms). During this temporal jitter, the screen was dark. We included this temporal jitter to allow use of the identical task in a magnetoencephalography study. At test, participants indicated with a button press whether the probe was the same as or did not match one of the sample scenes (50% match, 50% nonmatch trials). The probe scenes were equally likely to have been shown during the sample period in any temporal position (shown first or second for Load 2 trials and shown first, second, third, or fourth for Load 4 trials). All scenes were trial-unique, unless they were seen a second time at test (match). Variable-length delay periods and intertrial intervals were chosen to introduce differential overlap between subsequent sample, delay, and test periods to reduce collinearity. This approach was used in previous studies (Sakai and Passingham 2003; Cairo et al. 2004; Ranganath and D'Esposito 2005; Piekema et al. 2006; Schon et al. 2009). Subjects performed a total of 144 trials across 8 runs, with 9 Load 2 trials and 9 Load 4 trials per run.

fMRI Data Acquisition

Structural and functional imaging data were acquired on a 3.0 Tesla Siemens MAGNETOM Trio™ Tim® System scanner (Siemens AG, Medical Solutions) using a 12-channel Tim® Matrix head coil at the Athinoula A. Martinos Center for Biomedical Imaging, Massachusetts General Hospital, Charlestown, MA, USA. Structural scans consisted of 2 high-resolution T1-weighted magnetization prepared gradient echo (MP-RAGE) scans obtained using generalized autocalibrating partially parallel acquisitions (GRAPPA; Griswold et al. 2002) (TR = 2530 ms, TE = 3.44–3.48 ms, flip angle = 7°, number of slices = 176, field of view = 256 mm, and resolution = 1 × 1 × 1 mm^3). Functional data were acquired using T2*-sensitive gradient-echo, echo planar imaging (EPI) blood-oxygen level-dependent (BOLD) scans. Eight runs with 216 images per run were acquired during which subjects performed the task (TR = 2000 ms, TE = 34 ms, flip angle = 90°, 22 interleaved slices, field of view (FoV) = 96 mm, matrix size = 64 × 64, resolution = 1.5 × 1.5 × 1.5 mm^3, no interslice skip). A single T1-EPI scan was also obtained for each subject (TR = 18280 ms, TE = 52 ms, flip angle = 90°, field of view = 192 mm, matrix size = 128 × 128 mm^2, in-plane resolution = 1.5 mm^2, slice thickness = 1.5 mm, interslice skip = 0.3 mm, 90 interleaved slices, number of concatenations = 1) using the GRAPPA method. The EPI image slices were oriented approximately parallel to the long axis of the hippocampus, allowing inclusion of the hippocampal subfields (CA3/DG, CA1, subiculum), including the hippocampal tail, and the MTL subregions (EC, PrC, PHC, and amygdala) in the axial plane.

Data Preprocessing

Structural and functional data were preprocessed with SPM8 software (Wellcome Department of Cognitive Neurology) and MATLAB (MathWorks) routines. The images were reoriented such that the origin was 8 mm ventral to the anterior commissure. Preprocessing of BOLD data included correcting differences in slice timing, re-aligning to the first image collected within a series (motion correction), and unwarping to correct for image distortions due to susceptibility by movement interactions. The MP-RAGE structural and BOLD scans were coregistered to the T1-EPI. These preprocessing steps were then followed by cross-participant alignment of anatomical and BOLD images.

Cross-Participant Alignment

ROI-based regional cross-participant alignment (ROI-AL) procedures were used to optimize regional alignment of the hippocampal subfields and MTL cortices across all participants. This procedure allowed precise localization within these anatomically defined ROIs (Stark and Okado 2003; Miller et al. 2005; Yassa and Stark 2009). We used the same ROI-AL procedure and manual tracing protocol as in our previous work (Newmark et al. 2013). Hippocampal subfields (CA3/DG, CA1, subiculum) and extrahippocampal MTL regions (EC, PrC, PHC, and amygdala) were first manually delineated on each subject's anatomical MP-RAGE scan using techniques adapted for the visualization of these structures (Insausti et al. 1998; Pruessner et al. 2000, 2002).

Hippocampal boundaries included the fimbria, the inferior horn of the lateral ventricle, the uncus, and the quadrigeminal cistern. The subfields of the hippocampus were defined bilaterally using previously published methods (Kirwan and Stark 2007; Kirwan et al. 2007) and the Duvernoy atlas (Duvernoy 2005). The CA3 and dentate gyrus were combined to create the CA3/DG subfield, as the anatomical border could not be anatomically distinguished. Eight coronal slices identical or very similar to those depicted and described in the Duvernoy atlas were selected on each participant's average anatomical MR image for manual segmentation. Segmentation continued in 1-mm steps in both anterior and posterior direction from each of the 8 initial slices so that a smooth transition was created between slices. Landmarks for the delineation of the PrC, EC, and PHC included the gyrus of Schwalbe, the collateral sulcus, and the splenium of the corpus collosum.

Statistical Data Analysis

Our statistical analysis was identical to that of our previous whole-brain study using this task (Schon et al. 2009). Repeated-measures ANOVAs were used to investigate main effects of WM load (Load 2 and Load 4) and trial type (match and nonmatch) and interactions between WM load and trial type on behavioral performance (% correct, reaction time for correct trials). In addition, we also examined main effects of delay length and interactions between load and delay length on behavioral performance using repeated-measures ANOVAs. For analysis of BOLD activity

Figure 1. WM Task. During fMRI scanning, subjects performed a Sternberg task consisting of 72 trials per condition (Load 4 and Load 2) in each of 8 runs. Subjects viewed either 2 or 4 sequentially presented images of outdoor scenes (encoding phase), maintained the scenes across a 4- to 8-s variable-length delay period (maintenance phase), and determined whether a probe scene matched one of the previous images seen during that trial or was a nonmatch (test phase). Each trial ended with a variable-length fixation/ITI.

within the MTL, 16 regressors were created and convolved with the canonical hemodynamic response function for each combination of load (Load 2 and Load 4), event (encoding, maintenance, retrieval, and ITI/fixation), and accuracy (correct and incorrect). Delay periods were modeled as in Schon et al. (2009). Delay periods were modeled as short events of 4, 6, or 8-s duration. Additionally, the 6 movement parameters from the motion correction step were added as covariates to account for residual movement-related spurious activity. WM load effects were assessed by comparing Load 4 versus Load 2 for each phase of the task (encoding, maintenance, and retrieval) for correct trials only. Second-level analysis involved creating group-averaged SPMs by entering the contrast images into one-sample *t*-tests using subjects as a random factor. To correct for multiple comparisons, a cluster extent threshold of 20 contiguous voxels for a corrected threshold ($P < 0.05$) was determined using the AlphaSim algorithm (Forman et al. 1995) by running 10 000 Monte Carlo simulations at an uncorrected voxel-wise *P*-value of $P < 0.01$. Parameter estimates were extracted from peaks of regional activity using the Volumes toolbox extension for SPM5 and selectively averaged by load (Load 2 vs. Load 4) and by event (encoding vs. maintenance vs. retrieval) [http://sourceforge.net/projects/spmtools (Last accessed 21 January 2015)]. For visualization of parameter estimates, we averaged the extracted beta values across participants.

Results

Behavioral Results

There was no difference in accuracy (percent correct) between lower load trials and higher load trials (Mean ± Standard Error, Load 2 trials: 92.26 ± 2.21%, Load 4 trials: 91.04 ± 2.18%; $F_{1,14} = 1.13$, $P = 0.3$). As expected, reaction time analysis showed that participants answered faster to lower load trials than to higher load trials (Load 2 trials: 953.23 ± 34.0 ms; Load 4 trials: 1004.9 ± 30.6 ms; $F_{1,14} = 6.62$, $P = 0.022$). Participants performed better on nonmatch trials compared with match trials (Mean ± Standard Error, Nonmatch trials: 94.78 ± 2.07%, Match trials: 88.52 ± 2.34%; $F_{1,14} = 24.89$, $P < 0.01$), but there was no significant reaction time difference between nonmatch trials compared with match trials (Mean ± Standard Error, Nonmatch trials: 958.7 ± 32.6 ms, Match trials: 999.5 ± 32.4 ms; $F_{1,14} = 3.38$, $P = 0.08$). Additionally, there were no significant interactions between WM load and trial type (match/nonmatch) for reaction time and accuracy (reaction time: $F_{2,28} = 0.002$, $P = 0.966$; accuracy: $F_{2,28} = 1.13$, $P = 0.31$). We also conducted two-factor repeated-measures ANOVAs of load effects (Load 2 vs. Load 4) by delay length (4 s vs. 6 s vs. 8 s) for RT (correct trials) and accuracy to examine behavioral differences as a function of delay length. There were no main effects of delay length for both RT ($F_{2,13} = 0.840$, $P = 0.45$) and accuracy ($F_{2,13} = 0.093$, $P = 0.912$). In addition, there were no main effects of load for RT ($F_{1,14} = 0.412$, $P = 0.53$) and accuracy ($F_{1,14} = 1.215$, $P = 0.29$). Critically, the load effect by delay length interaction was not significant for both RT ($F_{2,28} = 0.128$, $P = 0.88$) and accuracy ($F_{2,28} = 0.060$, $P = 0.94$), suggesting that any fMRI effects observed for load should be independent of behavioral performance and of delay length.

fMRI Results

Load Effect during the Encoding Phase in CA1

When correct Load 4 trials were contrasted with correct Load 2 trials during the encoding phase (Fig. 2: Load 4 > Load 2, encoding phase), the group analysis showed significant activity within left CA1 (2 peaks: $T = 6.44$, $Z = 4.40$; $T = 4.55$, $Z = 3.55$, $P \leq 0.01_{corr}$), and right subiculum ($T = 4.87$, $Z = 3.71$, $P \leq 0.01_{corr}$). Additional areas activated for this contrast included left amygdala ($T = 4.16$; $Z = 3.34$, $P \leq 0.01_{corr}$) and right amygdala ($T = 4.84$, $Z = 3.70$, $P \leq 0.01_{corr}$). To illustrate the direction of the load effect in these regions during the encoding phase, we extracted parameter estimates (beta weights) from the peaks of these activation clusters and sorted them by encoding phase, delay period, and retrieval phase. These are shown in Figure 2.

Parahippocampal Areas but not Hippocampus Showed a Load Effect during the WM Delay

When correct Load 4 trials were contrasted with correct Load 2 trials during the maintenance phase (delay period) (Fig. 3: Load

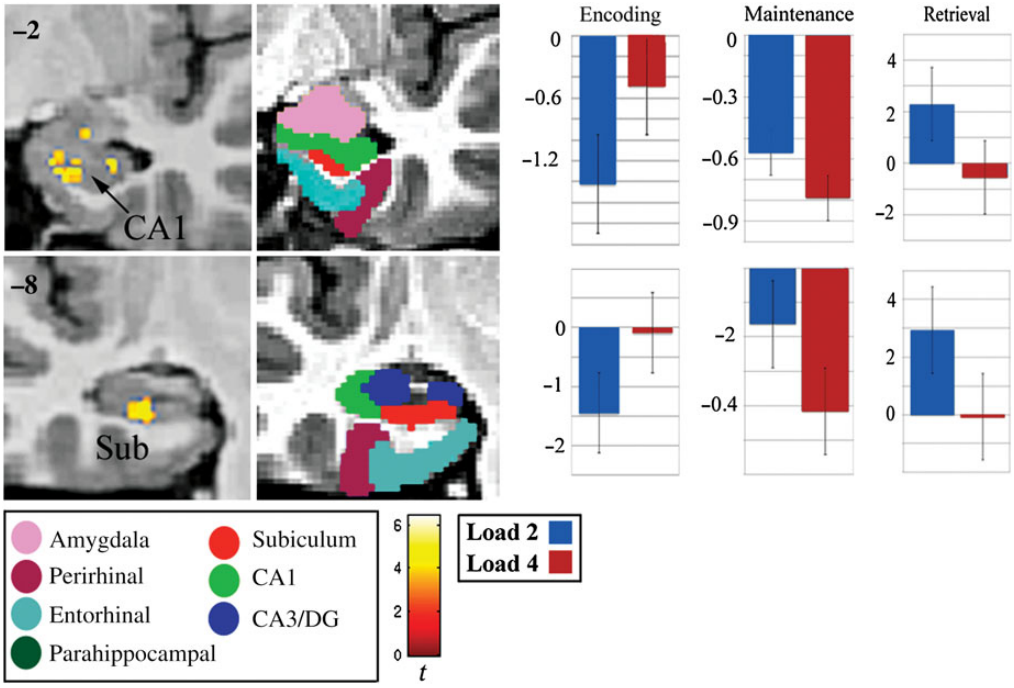

Figure 2. CA1 and subiculum show functional contribution while encoding a greater WM load (Load 4 > Load 2; encoding). The above images show thresholded statistical parametric maps for group-level activity superimposed on the representative structural template image, the corresponding segmented image, and graphs showing parameter estimates (beta weights) for Load 2 (blue) and Load 4 (red) for the encoding, maintenance, and retrieval (test) phases. The model segmentation is displayed to indicate the location of CA1 (light green), the subiculum (red), EC (light blue), PrC (violet), and PHC (dark green). Note that numbers correspond to y-coordinates, that is, the distance of each slice from the anterior commissure in millimeter (AC, y = 0 mm in Talairach coordinates; that is, regions posterior to the AC have negative y-values) and are indicated for each slice. Note that the coordinates describe a subject-specific space and are not in MNI or Talairach space. Images are displayed in "radiological" convention, with the right hemisphere displayed on the left side of the image.

4 > Load 2, delay), the group analysis showed significant activity within the right PHC (3 peaks: $T = 5.45$, $Z = 3.99$; $T = 4.61$, $Z = 3.58$; $T = 4.36$, $Z = 3.45$; $P \leq 0.01_{corr}$) and within a region composed of both the left PrC and EC ($T = 4.12$, $Z = 3.32$, $P \leq 0.01_{corr}$). Activity in these areas was greater for Load 4 than that for Load 2. To illustrate the direction of the load effect in these regions during the WM delay, we extracted parameter estimates (beta weights) from the peaks of these activation clusters and sorted them by encoding phase, delay period, and retrieval phase. These are shown in Figure 3.

Effects of WM Load during Retrieval in CA1

In our previous fMRI investigation that assessed WM load effects across the whole brain using the same task, but different subjects, we observed a load effect (Load 4 > Load 2) in a left anterior MTL region during retrieval (Schon et al. 2009). Greater activity during retrieval of the larger WM load (Load 4) compared with retrieval of the smaller WM load (Load 2) in that region was driven by nonmatch trials. Here, we examined whether we could replicate this result and extend it to the subfield level.

Across match and nonmatch trials, the load effect contrast at test (Load 4 > Load 2, retrieval) showed no significant areas of activity within the MTL. However, a load effect contrast for nonmatching scenes at test (Load 4 > Load 2, nonmatch, retrieval) showed significant activity within the right PHC (2 peaks: $T = 11.13$, $Z = 5.58$; $T = 5.12$, $Z = 3.78$; $P \leq 0.01_{corr}$), the left PHC (3 peaks: $T = 7.41$, $Z = 4.65$; $T = 5.70$, $Z = 4.03$; $T = 5.33$, $Z = 3.87$; $P \leq 0.01_{corr}$), and a region extending into right CA1 and CA3/DG ($T = 4.09$, $Z = 3.26$). A contrast of match trials (Load 4 Match > Load 2 Match, $P \leq 0.01_{corr}$) showed no significant activity within the MTL.

WM Load-Independent Effects

We also compared activity during the encoding, delay, and retrieval phases of the Sternberg task with that of the ITI (fixation) separately for each load. A contrast between Load 2 > ITI during the encoding phase showed activity within the PrC and PHC, whereas a contrast between Load 4 > ITI showed activity in the hippocampus (CA3/DG, CA1, and subiculum) as well as the EC, PrC, and PHC. During the delay period, both sets of contrasts showed activity within the EC, PrC, and PHC. During the retrieval phase, both sets of contrasts showed activity within the hippocampus (CA3/DG, CA1, and subiculum) as well as the EC, PrC, and PHC. Please see Supplementary Table 1, online, for details.

Discussion

A load effect during the WM task delay has previously been associated with a "limited-capacity" WM buffer linked to prefrontal and posterior cortical regions (Braver et al. 1997; Rypma et al. 1999; Jha and McCarthy 2000; Druzgal and D'Esposito 2003; see Schon et al. 2009, for a whole-brain study using the same cognitive task used here). In addition to these prefrontal and parietal contributions to WM, computational models have suggested that MTL regions also can act as a WM buffer (Lisman and Idiart 1995; Jensen and Lisman 1996, 1998, 2005; Koene and Hasselmo 2007). We examined activity within hippocampal subfields (CA3/DG, CA1, and subiculum) and neighboring medial temporal areas (PrC, EC, and PHC) while participants encoded, maintained, and retrieved information at 2 different WM loads. As predicted, we observed a WM load effect in CA1. We found that this WM load effect in CA1 was transient and did not sustain into the delay

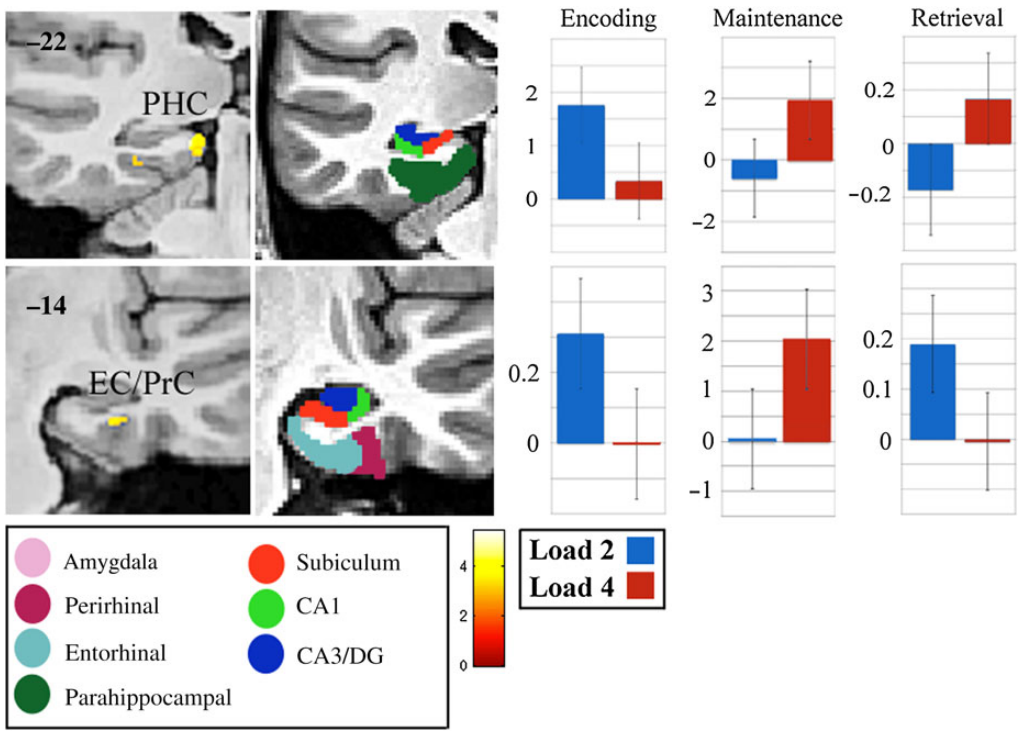

Figure 3. The entorhinal, perirhinal, and parahippocampal cortices show functional contribution while maintaining a greater WM load (Load 4 > Load 2; maintenance). The picture shows statistical parametric maps for group-level activity superimposed on the representative structural template image, the corresponding segmented image, and graphs showing parameter estimates (beta weights) for Load 2 (blue) and Load 4 (red) for encoding, maintenance, and retrieval (test) phases. The model segmentation is displayed to indicate the location of CA1 (light green), the subiculum (red), EC (light blue), PrC (violet), and PHC (dark green). Note that numbers correspond to *y*-coordinates, that is, the distance of each slice from the anterior commissure in millimeter (AC, *y* = 0 mm in Talairach coordinates; that is, regions posterior to the AC have negative *y*-values) and are indicated for each slice. Note that the coordinates describe a subject-specific space and are not in MNI or Talairach space. Images are displayed in "radiological" convention, with the right hemisphere displayed on the left side of the image.

period. In contrast, we found sustained delay-period activity within the EC, PrC, and PHC with greater WM load, consistent with our predictions.

Here, consistent with predictions from computational modeling work (Lisman and Idiart 1995; Jensen and Lisman 1996, 1998, 2005; Koene and Hasselmo 2007), we show that areas EC, PrC, and PHC are involved in active maintenance during WM in a load-dependent manner. Our findings extend other studies that use complementary techniques for investigating the neural correlates of WM maintenance. Single-unit recording studies have shown persistent neuronal firing in the EC indicating an important WM mechanism (Fransén et al. 2002; Hasselmo and Stern 2006). Furthermore, findings from cellular recording studies in animals have shown that persistent firing within the EC may underlie active maintenance across a brief delay period (Young et al. 1997; Egorov et al. 2002; Fransén et al. 2004; Yoshida et al. 2008). Additionally, using intracranial EEG, Axmacher et al. (2007) detected increased activity within the rhinal cortex during the maintenance of multiple items in subjects performing a Sternberg WM task. Complementary to our results, previous fMRI investigations have shown that sustained EC and PrC (Schon et al. 2004) and PHC activity (Schon et al. 2004; Axmacher et al. 2008) during the WM delay is associated with subsequent long-term memory performance. Based on this literature and the results presented here, we propose a role for the EC, PrC, and PHC in both WM maintenance and long-term memory encoding and suggest that these regions may serve as a buffer facilitating the transition of information from WM into long-term memory.

Previous findings from intracranial EEG recordings (Mainy et al. 2007) and an fMRI investigation (Kochan et al. 2011) have indicated that the hippocampus is recruited for encoding greater WM loads. We extend these findings to the subfield level by demonstrating a load-dependent activation in CA1 and subiculum during the encoding phase, suggesting a transient recruitment of these regions. The EC-CA1 pathway may play a role in episodic encoding when binding is required over brief temporal lags (Ryan and Cohen 2004; Hannula and Ranganath 2008; for review, see Langston et al. 2010). CA1 may have contributed to intraitem content binding when complex visual scenes were presented sequentially. A recent study using high-resolution fMRI has documented a linear increase in CA1 activity associated with novel features within an environment (Duncan et al. 2012), suggestive of a stimulus encoding and binding signal. Our work is consistent with a role of CA1 in encoding and feature binding. Such a binding signal in CA1, supportive of subsequent recollection, is consistent with the role of the hippocampus in binding item and context (reviewed in Diana et al. 2007). While this could not be tested here, a role for CA1 in binding item with context is consistent with our results given that we used complex visual scenes composed of items associated with the same context as stimuli. An alternative interpretation for this encoding load effect in CA1 and subiculum is that it may be influenced by differences in visual information processing or time on task rather than being purely due to encoding or intraitem content binding. We cannot distinguish between these alternative interpretations because we did not equate visual information processing by including 2 "filler" stimuli for the Load 2 condition, such as scrambled scenes. Both interpretations (encoding/intraitem content binding and visual information processing) are consistent with the idea that CA1 and subiculum are recruited when

participants attend to the distinctiveness of the stimuli during encoding (Carr et al. 2013).The results presented here suggest the EC/PrC and PHC, but not CA1, contribute to the active maintenance of higher WM loads. Previous fMRI studies have reported an absence of hippocampal activity while maintaining greater WM loads (Axmacher et al. 2007; Schon et al. 2009; Kochan et al. 2011). It is unclear whether the absence of a hippocampal load effect represents a true finding, because null results in fMRI studies could be due to poor model fit or use of spatial normalization techniques that align BOLD images to a standard template space without taking into account interindividual anatomical variations in small areas of interest, such as the hippocampus. In contrast to these studies, there is experimental evidence from intracranial EEG (van Vugt et al. 2010) and fMRI studies (Rissman et al. 2008) in support of such a role for the hippocampus. Our results demonstrate that the hippocampus was recruited in a load-dependent manner during the encoding phase but showed no sustained load-modulated activity during the delay. It may be possible that the hippocampus supports maintenance of multiple items only under some circumstances, for example, when interference between the stimuli that need to be maintained during the WM task delay is high. Reducing interference in the context of memory encoding is thought to depend on pattern separation, a hippocampus-dependent computational process (O'Reilly and McClelland 1994). Consistent with this idea, van Vugt et al. (2010) used highly similar synthetic, repeating faces as stimuli and observed a load effect during the delay period in the hippocampus, whereas the stimuli used in Axmacher et al. (2007), Schon et al. (2009), and Kochan et al. (2011) were more visually distinct or were novel, and none of these studies observed a load effect during the delay period in the hippocampus. WM for visually distinct stimuli or for those that are trial-unique or novel may not require pattern separation, because interference among the stimuli should be low. When interference among the stimuli that need to be maintained in WM is low, hippocampal activity may not change as a function of load. However, it is possible that functional connectivity between the hippocampus and extrahippocampal regions changes as a function of stimulus load to support long-term encoding without modulating hippocampal activity per se. If so, such a change would not be detectable with standard univariate statistical models such as those used in the studies cited earlier (Axmacher et al. 2007; Schon et al. 2009; Kochan et al. 2011) and used here. Support for this idea comes from a study by Rissman et al. (2008), who have shown that functional connectivity during the delay period between the fusiform face area and the hippocampus increased with increasing stimulus load for novel, distinct, face stimuli. It should be noted that the stimuli used in our current paradigm were unfamiliar outdoor scenes that likely did not require pattern separation or disambiguation as in our previous work (Newmark et al. 2013), where we observed delay-period activity in hippocampal subfields. Therefore, it may be possible that while the PrC/EC region and PHC are recruited to maintain a greater WM load of novel information, delay-period activity in CA1 and/or other hippocampal subfields may be modulated by WM load only if stimuli have overlapping features or are highly similar.

Activity during the shortest delay periods (4-s duration) may not be separable from sample-period activity due to collinearity between the sample phase and the delay period. A potential overlap between sample and delay periods is consistent with the idea of a WM buffer, because such a buffer should show ongoing encoding. We define ongoing encoding as stimulus encoding that starts during stimulus presentation and persists into the delay period. Consistent with the idea of ongoing encoding, Ranganath et al. (2005) have shown long-term memory effects during the early part of brief WM delays in the hippocampus, but not during the late part of these WM delays. Future studies are needed to examine time courses associated with ongoing encoding in regions supporting the putative WM buffer (EC/PrC, PHC).

Our results indicate that not only the EC/PrC region but also the PHC may act as a WM buffer based on our observation that activity in this region was increased with greater WM load during the WM task delay. While we did not have specific predictions regarding the role of this region as a WM buffer, it is not surprising given the role of the PHC and parahippocampal place area (PPA) in processing and mnemonic encoding of spatial scenes (Epstein et al. 1999, 2007; Awipi and Davachi 2008; Preston et al. 2010). The observed load effect in the PHC is inconsistent with previous neuroimaging studies (Ranganath et al. 2004; Axmacher et al. 2009; Schon et al. 2009). It may be possible that a load effect (high WM load > low WM load) is observed in the PHC only when the WM task requires encoding of spatial layouts or contextual information, as is the case for the complex visual scenes used in our study. Consistent with this idea, the PHC has been shown to respond more strongly to scenes than to faces or objects (Epstein and Kanwisher 1998; but see Diana et al. 2008). While Ranganath et al. (2004) and Schon et al. (2009) also used scenes as stimuli, their studies may not have been sensitive to a load effect given these 2 studies used a whole-brain approach that was not optimized for the MTL. A recent whole-brain fMRI study suggests delay-period activity in MTL cortex may be stimulus specific (Libby et al. 2014). Libby et al. (2014) reported delay-period activity in PrC and PHC supporting selective processing of object and spatial information embedded in complex visual scenes, respectively, although delay-period activity in the PrC was only marginally significant. Future studies are needed to determine the separate contributions of EC, PrC, PHC, and PPA subregion of the PHC to buffering different types of stimulus material (e.g., scenes vs. objects vs. faces) in WM.

Additionally, our results show that when nonmatch lures were identified at higher WM loads (Load 4 > Load 2, nonmatch retrieval), CA1, CA3/DG, and PHC showed increased activity. This result is consistent with our previous whole-brain fMRI study (Schon et al. 2009) that showed activity in a left anterior MTL area for this contrast. The results presented here extend these previous findings to the subfield level. Because the observed WM load effect at retrieval was specific to nonmatch trials, our results are also consistent with the purported role of the hippocampus in mismatch detection (Kumaran and Maguire 2007; Duncan et al. 2012) and suggest that successful lure rejection at higher loads may require scanning and comparing a presented item with multiple items represented within a WM buffer (see Schon et al. 2009).

Consistent with computational models (Jensen and Lisman 2005; Koene and Hasselmo 2007), we demonstrated that 1) load-dependent activity in CA1 and subiculum during WM is transient and that 2) EC, PrC, and PHC support the maintenance of higher cognitive loads across a brief temporal delay. This WM load effect in EC, PrC, and PHC implicates these regions in active maintenance, a WM process previously attributed to prefrontal and posterior association cortices. These results suggest a role for the EC/PrC and PHC as a WM buffer.

Supplementary Material

Supplementary material can be found at: http://www.cercor.oxfordjournals.org/.

Funding

This work was supported by the National Science Foundation Science of Learning Center (Grant numbers SMA-0835976 and SBE-0354378). We also acknowledge salary support for K.S. from NIH R00AG036845. Imaging was carried out at the Athinoula A. Martinos Center for Biomedical Imaging in Charlestown, Massachusetts, which receives support from the National Center for Research Resources (NCRR) Shared Instrumentation Grant Program and/or High-End Instrumentation Grant Program and NCRR Biomedical Technology Program at the National Institutes of Health (Grant numbers S10RR021110 and P41RR14075).

Notes

Conflict of Interest: None declared.

References

Awipi T, Davachi L. 2008. Content-specific source encoding in human medial temporal lobe. J Exp Psychol Learn Mem Cogn. 34:769–779.

Axmacher N, Haupt S, Cohen MX, Elger CE, Fell J. 2009. Interference of working memory load with long-term memory formation. Eur J Neurosci. 29:1501–1513.

Axmacher N, Mormann F, Fernández G, Cohen MX, Elger CE, Fell J. 2007. Sustained neural activity patterns during working memory in the human medial temporal lobe. J Neurosci. 27:7807–7816.

Axmacher N, Schmitz DP, Weinreich I, Elger CE, Fell J. 2008. Interaction of working memory and long-term memory in the medial temporal lobe. Cereb Cortex. 18:2868–2878.

Braver T, Cohen J, Nystrom L, Jonides J, Smith E, Noll D. 1997. A parametric study of prefrontal cortex involvement in human working memory. Neuroimage. 5:49–62.

Cairo TA, Liddle PF, Woodward TS, Ngan ETC. 2004. The influence of working memory load on phase specific patterns of cortical activity. Brain Res Cogn Brain Res. 21:377–387.

Carr VA, Engel SA, Knowlton BJ. 2013. Top-down modulation of hippocampal encoding activity as measured by high-resolution functional MRI. Neuropsychologia. 51:1829–1837.

Diana RA, Yonelinas AP, Ranganath C. 2008. High-resolution multi-voxel pattern analysis of category selectivity in the medial temporal lobes. Hippocampus. 18:536–541.

Diana RA, Yonelinas AP, Ranganath C. 2007. Imaging recollection and familiarity in the medial temporal lobe: a three-component model. Trends Cogn Sci. 11:379–386.

Druzgal TJ, D'Esposito M. 2003. Dissecting contributions of prefrontal cortex and fusiform face area to face working memory. J Cogn Neurosci. 15:771–784.

Duncan K, Ketz N, Inati SJ, Davachi L. 2012. Evidence for area CA1 as a match/mismatch detector: a high-resolution fMRI study of the human hippocampus. Hippocampus. 22: 389–398.

Duvernoy HM. 2005. The Human Hippocampus: Functional Anatomy, Vascularization and Serial Sections with MRI. 3rd ed. Berlin, Germany: Springer.

Egorov A, Hamam B, Fransén E, Hasselmo ME, Alonso AA. 2002. Graded persistent activity in entorhinal cortex neurons. Nature. 420:173–178.

Epstein R, Harris A, Stanley D, Kanwisher N. 1999. The parahippocampal place area: recognition, navigation, or encoding? Neuron. 23:115–125.

Epstein R, Kanwisher N. 1998. A cortical representation of the local visual environment. Nature. 392:598–601.

Epstein RA, Parker WE, Feiler AM. 2007. Where am I now? Distinct roles for parahippocampal and retrosplenial cortices in place recognition. J Neurosci. 27:6141–6149.

Felleman DJ, Van Essen DC. 1991. Distributed hierarchical processing in the primate cerebral cortex. Cereb Cortex. 1:1–47.

Fernández G, Brewer JB, Zhao Z, Glover GH, Gabrieli JD. 1999. Level of sustained entorhinal activity at study correlates with subsequent cued-recall performance: a functional magnetic resonance imaging study with high acquisition rate. Hippocampus. 9:35–44.

Forman SD, Cohen JD, Fitzgerald M, Eddy WF, Mintun MA, Noll DC. 1995. Improved assessment of significant activation in functional magnetic resonance imaging (fMRI): use of a cluster-size threshold. Magn Reson Med. 33:636–647.

Fransén E, Alonso AA, Dickson CT, Magistretti J, Hasselmo ME. 2004. Ionic mechanisms in the generation of subthreshold oscillations and action potential clustering in entorhinal layer II stellate neurons. Hippocampus. 14:368–384.

Fransén E, Alonso AA, Hasselmo ME. 2002. Simulations of the role of the muscarinic-activated calcium-sensitive nonspecific cation current INCM in entorhinal neuronal activity during delayed matching tasks. J Neurosci. 22:1081–1097.

Griswold MA, Jakob PM, Heidemann RM, Nittka M, Jellus V, Wang J, Kiefer B, Haase A. 2002. Generalized autocalibrating partially parallel acquisitions (GRAPPA). Magn Reson Med. 47:1202–1210.

Hannula DE, Ranganath C. 2008. Medial temporal lobe activity predicts successful relational memory binding. J Neurosci. 28:116–124.

Hasselmo ME, Stern CE. 2006. Mechanisms underlying working memory for novel information. Trends Cogn Sci. 10:487–493.

Insausti R, Amaral DG, Cowan WM. 1987. The entorhinal cortex of the monkey: II. Cortical afferents. J Comp Neurol. 264:356–395.

Insausti R, Juottonen K, Soininen H, Insausti AM, Partanen K, Vainio P, Laakso MP, Pitka A. 1998. MR volumetric analysis of the human entorhinal, perirhinal, and temporopolar cortices. Am J Neuroradiol. 19:659–671.

Jeneson A, Mauldin KN, Squire LR. 2010. Intact working memory for relational information after medial temporal lobe damage. J Neurosci. 30:13624–13629.

Jensen O, Lisman JE. 2005. Hippocampal sequence-encoding driven by a cortical multi-item working memory buffer. Trends Neurosci. 28:67–72.

Jensen O, Lisman JE. 1996. Novel lists of 7 +/– 2 known items can be reliably stored in an oscillatory short-term memory network: interaction with long-term memory. Learn Mem. 3:257–263.

Jensen O, Lisman JE. 1998. An oscillatory short-term memory buffer model can account for data on the Sternberg task. J Neurosci. 18:10688–10699.

Jha A, McCarthy G. 2000. The influence of memory load upon delay-interval activity in a working-memory task: an event-related functional MRI study. J Cogn Neurosci. 12:90–105.

Jochems A, Yoshida M. 2013. Persistent firing supported by an intrinsic cellular mechanism in hippocampal CA3 pyramidal cells. Eur J Neurosci. 38:2250–2259.

Kirwan CB, Jones CK, Miller MI, Stark CEL. 2007. High-resolution fMRI investigation of the medial temporal lobe. Hum Brain Mapp. 28:959–966.

Kirwan CB, Stark CEL. 2007. Overcoming interference: an fMRI investigation of pattern separation in the medial temporal lobe. Learn Mem. 14:959–966.

Klink R, Alonso A. 1997. Ionic mechanisms of muscarinic depolarization in entorhinal cortex layer II neurons. J Neurophysiol. 77:1829–1843.

Knauer B, Jochems A, Valero-Aracama MJ, Yoshida M. 2013. Long-lasting intrinsic persistent firing in rat CA1 pyramidal cells: a possible mechanism for active maintenance of memory. Hippocampus. 23:820–831.

Kochan NA, Valenzuela M, Slavin MJ, McCraw S, Sachdev PS, Breakspear M. 2011. Impact of load-related neural processes on feature binding in visuospatial working memory. PLoS One. 6:e23960.

Koene RA, Gorchetchnikov A, Cannon RC, Hasselmo ME. 2003. Modeling goal-directed spatial navigation in the rat based on physiological data from the hippocampal formation. Neural Netw. 16:577–584.

Koene RA, Hasselmo ME. 2007. First-in-first-out item replacement in a model of short-term memory based on persistent spiking. Cereb Cortex. 17:1766–1781.

Kumaran D, Maguire EA. 2007. Match mismatch processes underlie human hippocampal responses to associative novelty. J Neurosci. 27:8517–8524.

Langston RF, Stevenson CH, Wilson CL, Saunders I, Wood ER. 2010. The role of hippocampal subregions in memory for stimulus associations. Behav Brain Res. 215:275–291.

Lee ACH, Rudebeck SR. 2010. Investigating the interaction between spatial perception and working memory in the human medial temporal lobe. J Cogn Neurosci. 22:2823–2835.

Libby LA, Hannula DE, Ranganath C. 2014. Medial temporal lobe coding of item and spatial information during relational binding in working memory. J Neurosci. 34:14233–14242.

Lisman J, Idiart M. 1995. Storage of 7+/-2 short-term memories in oscillatory subcycles. Science. 267:1512–1515.

Mainy N, Kahane P, Minotti L, Hoffmann D, Bertrand O, Lachaux J-P. 2007. Neural correlates of consolidation in working memory. Hum Brain Mapp. 28:183–193.

McGaughy J, Koene RA, Eichenbaum H, Hasselmo ME. 2005. Cholinergic deafferentation of the entorhinal cortex in rats impairs encoding of novel but not familiar stimuli in a delayed nonmatch-to-sample task. J Neurosci. 25: 10273–10281.

Miller MI, Beg MF, Ceritoglu C, Stark C. 2005. Increasing the power of functional maps of the medial temporal lobe by using large deformation diffeomorphic metric mapping. Proc Natl Acad Sci USA. 102:9685–9690.

Navaroli VL, Zhao Y, Boguszewski P, Brown TH. 2012. Muscarinic receptor activation enables persistent firing in pyramidal neurons from superficial layers of dorsal perirhinal cortex. Hippocampus. 22:1392–1404.

Newmark RE, Schon K, Ross RS, Stern CE. 2013. Contributions of the hippocampal subfields and entorhinal cortex to disambiguation during working memory. Hippocampus. 23:467–475.

Nichols EA, Kao Y-C, Verfaellie M, Gabrieli JD. 2006. Working memory and long-term memory for faces: Evidence from fMRI and global amnesia for involvement of the medial temporal lobes. Hippocampus. 16:604–616.

O'Reilly RC, McClelland JL. 1994. Hippocampal conjunctive encoding, storage, and recall: avoiding a trade-off. Hippocampus. 4:661–682.

Olsen RK, Nichols EA, Chen J, Hunt JF, Glover GH, Gabrieli JDE, Wagner AD. 2009. Performance-related sustained and anticipatory activity in human medial temporal lobe during delayed match-to-sample. J Neurosci. 29:11880–11890.

Pessoa L, Gutierrez E, Bandettini PA, Ungerleider LG. 2002. Neural correlates of visual working memory: fMRI amplitude predicts task performance. Neuron. 35:975–987.

Piekema C, Kessels RPC, Mars RB, Petersson KM, Fernández G. 2006. The right hippocampus participates in short-term memory maintenance of object-location associations. Neuroimage. 33:374–382.

Preston AR, Bornstein AM, Hutchinson JB, Gaare ME, Glover GH, Wagner AD. 2010. High-resolution fMRI of content-sensitive subsequent memory responses in human medial temporal lobe. J Cogn Neurosci. 22:156–173.

Pruessner JC, Köhler S, Crane J, Pruessner M, Lord C, Byrne A, Kabani N, Collins DL, Evans AC. 2002. Volumetry of temporopolar, perirhinal, entorhinal and parahippocampal cortex from high-resolution MR images: considering the variability of the collateral sulcus. Cereb Cortex. 12:1342–1353.

Pruessner JC, Li LM, Serles W, Pruessner M, Collins DL, Kabani N, Lupien S, Evans AC. 2000. Volumetry of hippocampus and amygdala with high-resolution MRI and three-dimensional analysis software: minimizing the discrepancies between laboratories. Cereb Cortex. 10:433–442.

Ranganath C, Cohen MX, Brozinsky CJ. 2005. Working memory maintenance contributes to long-term memory formation: neural and behavioral evidence. J Cogn Neurosci. 17:994–1010.

Ranganath C, D'Esposito M. 2005. Directing the mind's eye: prefrontal, inferior and medial temporal mechanisms for visual working memory. Curr Opin Neurobiol. 15:175–182.

Ranganath C, DeGutis J, D'Esposito M. 2004. Category-specific modulation of inferior temporal activity during working memory encoding and maintenance. Brain Res Cogn Brain Res. 20:37–45.

Ranganath C, Esposito MD. 2001. Medial temporal lobe activity associated with active maintenance of novel information. Neuron. 31:865–873.

Rissman J, Gazzaley A, D'Esposito M. 2008. Dynamic adjustments in prefrontal, hippocampal, and inferior temporal interactions with increasing visual working memory load. Cereb Cortex. 18:1618–1629.

Ryan J, Cohen NJ. 2004. Processing and short-term retention of relational information in amnesia. Neuropsychologia. 42:497–511.

Rypma B, Prabhakaran V, Desmond J, Glover GH, Gabrieli JD. 1999. Load-dependent roles of frontal brain regions in the maintenance of working memory. Neuroimage. 9:216–226.

Sakai K, Passingham RE. 2003. Prefrontal interactions reflect future task operations. Nat Neurosci. 6:75–81.

Schon K, Hasselmo ME, LoPresti ML, Tricarico MD, Stern CE. 2004. Persistence of parahippocampal representation in the absence of stimulus input enhances long-term encoding: a functional magnetic resonance imaging study of subsequent memory after a delayed match-to-sample task. J Neurosci. 24:11088–11097.

Schon K, Quiroz YT, Hasselmo ME, Stern CE. 2009. Greater working memory load results in greater medial temporal activity at retrieval. Cereb Cortex. 19:2561–2571.

Schon K, Ross RS, Hasselmo ME, Stern CE. 2013. Complementary roles of medial temporal lobes and mid-dorsolateral prefrontal cortex for working memory for novel and familiar trial-unique visual stimuli. Eur J Neurosci. 37:668–678.

Shrager Y, Levy DA, Hopkins RO, Squire LR. 2008. Working memory and the organization of brain systems. J Neurosci. 28:4818–4822.

Staresina BP, Duncan KD, Davachi L. 2011. Perirhinal and parahippocampal cortices differentially contribute to later recollection of object- and scene-related event details. J Neurosci. 31:8739–8747.

Stark CEL, Okado Y. 2003. Making memories without trying: medial temporal lobe activity associated with incidental memory formation during recognition. J Neurosci. 23:6748–6753.

Sternberg S. 1966. High-speed scanning in human memory. Science. 153:652–654.

Suzuki WA, Amaral DG. 1994. Topographic organization of the reciprocal connections between the monkey entorhinal cortex and the perirhinal and parahippocampal cortices. J Neurosci. 14:1856–1877.

Suzuki WA, Miller EK, Desimone R. 1997. Object and place memory in the macaque entorhinal cortex. J Neurophysiol. 78:1062–1081.

Tahvildari B, Fransén E, Alonso AA, Hasselmo ME. 2007. Switching between "On " and "Off" states of persistent activity in lateral entorhinal layer III neurons. Hippocampus. 17:257–263.

Van Hoesen GW, Pandya DN. 1975a. Some connections of the entorhinal (area 28) and perirhinal (area 35) cortices of the rhesus monkey. I. Temporal lobe afferents. Brain Res. 95:1–24.

Van Hoesen GW, Pandya DN. 1975b. Some connections of the entorhinal (area 28) and perirhinal (area 35) cortices of the rhesus monkey. III. efferent connections. Brain Res. 95:39–59.

Van Vugt MK, Schulze-Bonhage A, Litt B, Brandt A, Kahana MJ. 2010. Hippocampal gamma oscillations increase with memory load. J Neurosci. 30:2694–2699.

Witter M, Van Hoesen GW, Amaral DG. 1989. Topographical organization of the entorhinal projection to the dentate gyrus of the monkey. J Neurosci. 9:216–228.

Yassa MA, Stark CEL. 2009. A quantitative evaluation of cross-participant registration techniques for MRI studies of the medial temporal lobe. Neuroimage. 44:319–327.

Yoshida M, Fransén E, Hasselmo ME. 2008. mGluR-dependent persistent firing in entorhinal cortex layer III neurons. Eur J Neurosci. 28:1116–1126.

Young BJ, Otto T, Fox GD, Eichenbaum H. 1997. Memory representation within the parahippocampal region. J Neurosci. 17:5183–5195.

Zarahn E, Rakitin B, Abela D, Flynn J, Stern Y. 2005. Positive evidence against human hippocampal involvement in working memory maintenance of familiar stimuli. Cereb Cortex. 15:303–316.